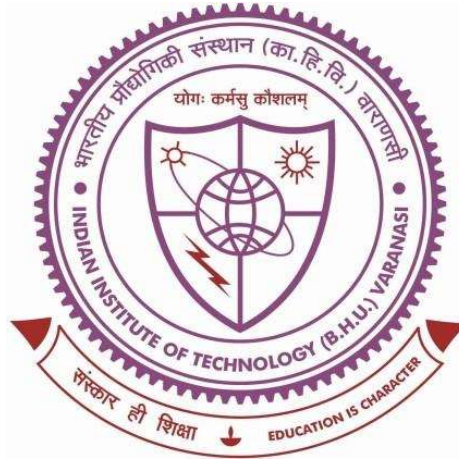


Sustainable Micromilling of Ti6Al4V alloy Using Different Eco-friendly Lubricants with MQL and coated tools



Thesis submitted in partial fulfillment for the
Award of Degree

Doctor of Philosophy

By

Ashutosh Roushan

DEPARTMENT OF MECHANICAL ENGINEERING
INDIAN INSTITUTE OF TECHNOLOGY
(BANARAS HINDU UNIVERSITY)
VARANASI - 221005

Roll No. 15131504

2022

CERTIFICATE

It is certified that the work contained in the thesis titled "*Sustainable Micromilling of Ti6Al4V alloy Using Different Eco-friendly Lubricants with MQL and Coated Tools*" by "*ASHUTOSH ROUSHAN*" has been carried out under my supervision and that this work has not been submitted elsewhere for a degree. A thesis submitted in partial fulfillment for the Award of Degree.

It is further certified that the student has fulfilled all the requirements of Comprehensive Examination, Candidacy, and SOTA for the award of Ph.D. Degree.



Supervisor
Dr. U. S. Rao

(Associate Professor)

Department of Mechanical Engineering
Indian Institute of Technology
(Banaras Hindu University),
Varanasi-221005, INDIA

Dr. U. SRINIVAS RAO
Associate Professor
Mechanical Engineering Department
Indian Institute of Technology (BHU)
Varanasi-221005

DECLARATION BY THE CANDIDATE

I, "**ASHUTOSH ROUSHAN**", certify that the work embodied in this thesis is my own bonafide work and carried out by me under the supervision of "**Dr. U. S. RAO**" from "**DECEMBER 2015**" to "**NOVEMBER 2022**", at the "**DEPARTMENT OF MECHANICAL ENGINEERING**", Indian Institute of Technology (BHU), Varanasi, India. The matter embodied in this thesis has not been submitted for the award of any other degree/diploma. I declare that I have faithfully acknowledged and given credits to the research workers wherever their works have been cited in my work in this thesis. I further declare that I have not wilfully copied any other's work, paragraphs, text, data, results, *etc.*, reported in journals, books, magazines, reports dissertations, theses, *etc.*, or available at websites and have not included them in this thesis and have not cited as my own work.

Date: 8/6/2023
Place: Varanasi

Ashutosh Roushan
(**ASHUTOSH ROUSHAN**)

CERTIFICATE BY THE SUPERVISOR

It is certified that the above statement made by the student is correct to the best of my knowledge

Supervisor 

Dr. U. S. Rao

(Associate Professor)

IIT (BHU), Varanasi, INDIA

Associate Professor

Deptt. of Mechanical Engg.

Indian Institute of Technology

Varanasi-221005


Signature of Head of Department

Department of Mechanical Engineering,

विभागाध्यक्ष / HEAD

यांत्रिक अभियान्त्रिकी विभाग / Deptt. of Mechanical Engg.

भारतीय प्रौद्योगिकी संस्थान / Indian Institute of Technology

(कानपुर/वि०/B.H.U.)

वाराणसी / Varanasi

COPYRIGHT TRANSFER CERTIFICATE

Title of the Thesis: *“Sustainable Micromilling of Ti6Al4V alloy Using Different Eco-friendly Lubricants with MQL and Coated Tools”*

Name of the Student: Ashutosh Roushan

Copyright Transfer

The undersigned hereby assigns to the Indian Institute of Technology (Banaras Hindu University), Varanasi all rights under copyright that may exist in and for the above thesis submitted for the award of the **Doctor of Philosophy**.

Date: 8/6/2023
Place: Varanasi

Ashutosh Roushan
(Ashutosh Roushan)

Note: However, the author may reproduce or authorize others to reproduce material extracted verbatim from the thesis or derivative of the thesis for the author's personal use provided that the source and the Institute's copyright notice are indicated.

DEDICATED

To

My Teachers

&

My Family Members

TABLE OF CONTENTS

<i>CONTENTS</i>		Page No.
<i>ABSTRACT</i>		i
<i>ACKNOWLEDGEMENT</i>		iv
<i>LIST OF FIGURES</i>		vi
<i>LIST OF TABLES</i>		xiv
<i>LIST OF ABBREVIATIONS/SYMBOLS</i>		xv
Chapter 1	INTRODUCTION	1-8
1.1	Micromilling background	1
1.2	Sustainable machining techniques	4
1.3	Motivation	5
1.4	Research objectives	6
1.5	Thesis outlines	7
Chapter 2	LITERATURE REVIEW	9-38
2.1	Machining mechanics in micromilling	9
2.1.1	Size effect and minimum undeformed chip thickness	11
2.1.2	Difficulties in micromachining of titanium alloys	13
2.2	Process performances in micro-end milling	14
2.2.1	Burr formation	14
2.2.2	Tool wear	18
2.2.3	Surface roughness	18
2.2.4	Cutting forces	19

2.2.5	Cutting temperature	20
2.3	Effect of the thin film-coated tool in micromachining	21
2.4	Metal cutting fluids (MCFs) and sustainable techniques	26
2.4.1	Lubrication mechanism of nanoparticles as lubricant additives	28
2.4.2	Utilization of cutting fluids and nanofluids in micromachining with MQL	29
2.5	Influence of MQL parameters on machining performances	35
2.6	Gaps in knowledge and need for research	36
Chapter 3	Experimental setup	39-46
3.1	Work material and cutting tools	39
3.2	Experimental setup	41
3.3	Summary	46
Chapter 4	Performance evaluation of tool coatings and nanofluid MQL on the micro-machinability of Ti-6Al-4V	47-84
4.1	Experimental procedure	47
4.1.1	Work material, coated tool, and MQL assisted micromilling	47
4.1.2	Nano-cutting fluids: preparation and characterization	53
4.1.3	Wettability analysis	57
4.2	Results and discussion	58
4.2.1	Tool wear	58
4.2.2	Cutting forces	69
4.2.3	Surface roughness	74
4.2.4	Burr formation and surface topography	77
4.3	Summary	82

Chapter 5	Tribological aspects and size effect in micromilling of Ti-6Al-4V alloy using vegetable oil nanofluids with minimum quantity lubrication	85-120
5.1	Experimental procedure	86
5.1.1	Work material, coated tool, and MQL assisted micromilling	86
5.1.2	Characterization of nanoparticles and nanofluids	89
5.1.3	Micro-mist droplets measurement	93
5.1.4	Wettability test	94
5.1.5	Tribology tests	95
5.2	Results and discussions	98
5.2.1	Evaluation of tool wear and wear mechanisms	98
5.2.2	Specific cutting force	106
5.2.3	Burr formation	110
5.2.4	Surface roughness and surface topography	114
5.3	Summary	118
Chapter 6	Application of eco-friendly emulsions with different flow rates during MQL assisted micromilling of Ti6Al4V	121-140
6.1	Experimental procedure	121
6.1.1	Work material and MQL assisted micromilling	121
6.2	Results and discussion	124

6.2.1	Tribology tests and micromilling forces	124
6.2.2	Analysis of surface quality	129
6.3	Summary	138
Chapter 7	Conclusion and Future Research Initiatives	141-146
7.1	Conclusion	141
7.1.1	External Delivery Using CuO-Enhanced Environmentally-Benign water-based Cutting Fluids and utilization of different coated microtools	141
7.1.2	External Delivery Using CuO and MoS ₂ -Enhanced Environmentally-Benign vegetable oil-based cutting fluids	142
7.1.3	Variation of emulsions supply at different rotational speeds to enhance machining performance	144
7.2	Future Research Initiatives	145
	References	147
	List of publications from thesis	158

ABSTRACT

The increased multi-functionality of today's very precise microstructures/components, along with a gradual decline in weight and cost, has made them more attractive in various industries. Several products and features, including micro-slots, microneedles, micro-pins, micro-barbs, microfluidic devices, and microtextured surfaces on biomedical implants, were developed using titanium-based alloys, particularly Ti6Al4V alloy, which found extensive use in the aerospace and biomedical areas. Micromilling used to manufacture complex 3D micro parts and features such as watch making, miniature heat exchanger, micro mould, micro valves, lab-on-chip and micro injection nozzles in a variety of materials. Micro milling is the most flexible process that fabricates three-dimensional microfeatures or components. Moreover, because of the micro tool's minimal diameter (1-999 μm), many factors, including size effect, minimum uncut chip thickness effect, tool run-out, and plowing, impact the chip formation process. The Ti6Al4V alloy's poor thermal conductivity and heat buildup properties promote rapid tool wear, lower the quality of the finished surface, and make it more difficult to machine the material. Two solutions to this problem include introducing hard, wear-resistant coated tools and sustainable cooling and lubrication systems. As an outcome, it is believed that the application of both nanofluid based MQL and coated tools together can enhance the micro-machinability even more, but no related studies have been discovered presently. Also, there is a scope to investigate the impact of hybrid nanofluids (nanofluids where constituent of nanomaterials is more than one) in micro milling of Ti6Al4V. This research uses coated tools and minimum quantity lubrication with eco-friendly vegetable oil and its nanofluids, water-based nanofluids, and vegetable oil-water emulsion to improve micromilling performance. Thus, micromilling tests were performed with uncoated WC and two different coated tools: AlTiN and TiAlN coated

micro end mills. First, the various volume concentrations of CuO nanofluids are made, and their stability, wettability, and viscosity are assessed in reducing the gap. Experimental research was done to evaluate the impacts of the various systems on cutting force, tool wear, surface roughness, and burr formation. Tool wear is analyzed in terms of percentage diameter reduction and various tool wear mechanism such as adhesion, abrasion, grains pull-out, edge chipping, built-up edge, and coating delamination. Uncoated tool in dry conditions is subjected to severe tool wear due to combined influence of residual stress, cyclic loading and abrasion. AlTiN coated tool shows better machining performance in dry conditions due to a lower coefficient of friction and higher hardness. The surface morphology of uncoated and coated tools after machining under 1 vol% CuO nanofluids MQL conditions shows the absence of built-up edge and material adhesion. This happens due to the enhanced lubrication and cooling rate of nanofluids with an increased volume percentage of CuO nanoparticles. The outcomes demonstrated that the AlTiN-coated WC micro end-mill with 0.25 vol% CuO water-based nanofluids significantly reduced surface roughness and cutting forces. Minimum average top burr widths of 9.93 μm and 10.58 μm were found in up milling and down milling, with AlTiN and TiAlN coated WC tools under 0.25 vol% CuO nanofluid based MQL. Using uncoated and coated tools, MQL generated a consistent surface topography with fewer defects.

Another experiment was done to determine how effectively minimum quantity lubrication (MQL) would work by adding CuO and MoS₂ nanoparticles separately and mixing them together with vegetable oil. Further, these nanofluids are utilized in the micromilling of Ti6Al4V under plowing (0.3 $\mu\text{m}/\text{tooth}$ feed) and shearing (4 $\mu\text{m}/\text{tooth}$ feed) conditions. Results showed that hybrid CuO-MoS₂ nanofluids significantly improved surface finish due to the combined effect of rolling and shearing by CuO

nanoparticles and MoS₂ nanoplatelets. Viscosity, wettability, and coefficient of friction of pure soybean oil and mono and hybrid nanofluids are characterized. The results demonstrated that the addition of CuO and MoS₂ nanoparticles improved the wettability, viscosity, and tribological properties of the cutting fluid and provided a considerable improvement over dry conditions in tool wear, specific cutting force, burr formation, and surface roughness. CuO nanofluid-based-MQL exhibited the best result in the shearing-dominant region by reducing tool wear, burrs, and specific cutting force due to the best wetting nature and rolling action. The surface roughness at 0.3 $\mu\text{m}/\text{tooth}$ feed was lessened by about 34.8%, 50.1%, 37.6% and 59.9% using soybean oil MQL, CuO, MoS₂ and CuO-MoS₂ nanofluids MQL compared to dry conditions. Similarly, at 4 $\mu\text{m}/\text{tooth}$ feed surface roughness is reduced by about 34.8%, 50.1%, 37.6% and 59.9% using soybean oil MQL, CuO, MoS₂ and CuO-MoS₂ nanofluids MQL compared to dry conditions. For the shearing regime at 4 $\mu\text{m}/\text{tooth}$ feed, CuO and MoS₂ NF-MQL were found more effective for adhesion wear than vegetable oil MQL and dry conditions. However, for plowing regime at 0.3 $\mu\text{m}/\text{tooth}$ feed, pure soybean oil MQL reduces tool adhesion through proper lubrication. Surface topography has also shown smoother with fewer feed marks and surface defects for hybrid nanofluids due to synergistic effect produced by the spherical CuO and the lamellar MoS₂, as well as by the improvement in the effectiveness of the interfacial slipping action mechanism.

The objective of the final section of this study was to select the appropriate emulsion for Ti6Al4V alloy micromilling at a specific flow rate and a range of spindle speeds, as well as to evaluate micromilling performance in terms of cutting force, burr formation, surface roughness, and surface topography. It has been observed that significant cutting force, surface roughness, and burr reduction occur using emulsions (paraffin oil-water emulsion and soybean oil-water emulsion) at different flow rates.

ACKNOWLEDGEMENT

The author is pleased to express his sincere thanks and gratitude beyond words to his supervisor Dr. U. S. Rao for his consistent help, encouragement and valuable discussions during the entire period of his research work. The author would not have been able to complete the thesis without his utmost involvement and invaluable efforts. He motivated the author to pursue research problems and the need for persistent effort to accomplish the goal. The author is truly indebted to him.

Besides supervisors, the author would like to thank his RPEC members, Dr. Meghanshu Vashista and Dr. C. K. Behera for their insightful comments and encouragement. The author is very much thankful to Prof. Karali Patra, Mechanical Engineering Department, IIT Patna, for providing Experimental facility. The author acknowledges his deep sense of gratitude to the current and former Heads of the Department of Mechanical Engineering for providing all the research facilities to accomplish his research in the Department successfully. The author has an immense sense of gratitude to all the faculty members of the Department of Mechanical Engineering, IIT (BHU), Varanasi for their cooperation and inspiration.

The author is grateful to all his friends Mr. Priyabrata Sahoo, Mr. Homender Kumar, Mr. Sooraj Singh Rawat, Mr. Akash Awale, Mr. Ashwani Ranjan, Mr. Miraz, Mr. Asgar Shakil Khan, Mr. Jitendra Kumar Singh, Mr. B. Rajak, Mr. Ajit Jha, Mr. Anupam Tiwari, Mr. Adarsh and Mr. Partha Sarathi Mallick, Mr. Nitesh Dubey and seniors especially Mr. Siddharth Yadav and Mr. Manish Deo for their constant encouragement, making joyful and memorable life being with him in moments of happiness and difficulties at IIT (BHU), Varanasi. The author is also thankful to all the lab and office staff of the department, especially Mr. Rajendra Prasad (Production lab).

The author would also like to express his immense gratitude to his parents Smt. Lilawati Devi and Shri Ram Gopal Prasad, wife Chanda Kumari, lovely Son Chinu, and other family members for their unconditional support and encouragement, to pursue his interest. The author also wishes to thank all those who have helped in any manner during the course of his research work.

(ASHUTOSH ROUSHAN)

LIST OF FIGURES

Fig. 1.1	Peer-reviewed papers about significant mechanical micromachining systems have increased over the last two decades	2
Fig. 1.2	Diagram of a milling tool cutting a workpiece	4
Fig. 1.3	Manufacturing sustainability	5
Fig. 2.1	Photographs illustrating the difference in scale between conventional milling (left) and micro-milling	10
Fig. 2.2	Comparison between tool edge radius, grain size, and undeformed chip thickness in traditional milling and micromilling	11
Fig. 2.3	Diagram of the processes for removing microchips in (a) elastic, (b) elastic-plastic, (c) plastic regime	12
Fig. 2.4	Stages of top burr formation: Initiation, propagation, and formation	15
Fig. 2.5	Diagram of Poisson burr, tear burr, and rollover burr	16
Fig. 2.6	Types of milling burr according to locations	17
Fig. 2.7	Five types of burrs in face milling	17
Fig. 2.8	Measurement of (a) flank wear (b) tool diameter reduction, and (c) change in edge radius	19
Fig. 2.9	The schematic of micromilling force in complete immersion milling	20
Fig. 2.10	SEM images of chips adhering to the cutting edges of coated tools	24
Fig. 2.11	Three-dimensional topographic images of surfaces machined by uncoated, DLC, AlTiN, and TiAlN + AlCrN coated micro mills	25
Fig. 2.12	Three-dimensional topographic images of surfaces machined by TiAlN + WC/C and AlCrN coated micro mills	26

Fig. 2.13	Health hazards related to uses of minerals oils	28
Fig. 2.14	Schematic illustration of (a) rolling, (b) self-repairing or mending, (c) polishing, and (d) tribo-film formation mechanisms	29
Fig. 3.1	Microstructure of Ti6Al4V alloy	39
Fig. 3.2	EDS profile for Ti6Al4V	40
Fig. 3.3	End view of fresh solid carbide micro end-mill	41
Fig. 3.4	(a) Schematic diagram of setup for micro milling and (b) MQL setup with its accessories attached to micromachine	43
Fig. 4.1	DT 110 micromachine with MQL setup	48
Fig. 4.2	SEM images of fresh TiAlN coated WC micro end-mill (a) bottom view, (b) cutting edge radius, (c) side view	49
Fig. 4.3	(a) Microstructure and (b) XRD of Ti6Al4V alloy	50
Fig. 4.4	Slots machined on Ti-grade 5 work material at (a) 1 vol% CuO nanofluid MQL condition, (b) 0.25 vol% CuO nanofluid MQL (c) dry and (d) pure MQL (deionized water)	52
Fig. 4.5	Image of a cross-section showing space between two consecutive micro-grooves	53
Fig. 4.6	(a) SEM image of CuO nanoparticles (b) XRD of CuO nanoparticles (c) size of nanoparticles versus the number of counts	55
Fig. 4.7	Zeta potential of CuO nanofluids at (a) 0.1 vol% (b) 0.25 vol% (c) 0.5 vol% (d) 0.75 vol% concentration	56
Fig. 4.8	Size distribution of aggregated CuO nanoparticles in deionized water at (a) 0.1 vol (b) 0.25 vol% (c) 0.5 vol% (d) 0.75 vol% concentration	56

- Fig. 4.9 (a) Wettability of nanofluids droplet on the solid substrate (b) pictorial view of contact angle measurement setup 57
- Fig. 4.10 Examples of drop pendants of deionized water and CuO nanofluids on uncoated surface at (a) 0 vol% (b) 0.1 vol% (c) 0.25 vol% (d) 0.5 vol% (e) 0.75 vol% (f) 1 vol%, TiAlN coated surface at (g) 0 vol% (h) 0.1 vol% (i) 0.25 vol% (j) 0.5 vol% (k) 0.75 vol% (l) 1 vol% and AlTiN coated surface at (m) 0 vol% (n) 0.1 vol% (o) 0.25 vol% (p) 0.5 vol% (q) 0.75 vol% (r) 1 vol% 60
- Fig. 4.11 SEM images of (a) uncoated, (b) TiAlN coated, and (c) AlTiN coated WC micro mills in dry condition with (d) EDS analysis of AlTiN coated cutting edge after cutting process of 450 mm length 61
- Fig. 4.12 SEM images of (a) uncoated, (b) AlTiN coated, and (c) TiAlN coated WC micro end-mills with an enlarged view of both cutting edges in pure MQL condition (deionized water) after 450 mm cutting length 63
- Fig. 4.13 EDS results of (a) uncoated, (b) AlTiN coated, and (c) TiAlN coated WC micro end-mills in pure MQL condition after 450 mm cutting length 64
- Fig. 4.14 SEM images of (a) uncoated, (b) AlTiN coated, and (c) TiAlN coated WC micro mills in nanofluid MQL condition with 0.25 vol% CuO after 450 mm cutting length 65
- Fig. 4.15 EDS results of (a) uncoated, (b) AlTiN coated, and (c) TiAlN coated WC micro end-mills in 0.25 vol% CuO nano-MQL condition after 450 mm cutting length 67
- Fig. 4.16 SEM images of (a) uncoated, (b) AlTiN coated, and (c) TiAlN coated WC micro end-mills in nano-MQL condition with 1 vol% CuO after 450 mm cutting length 68

Fig. 4.17	EDS results of (a) uncoated and (b) TiAlN coated WC micro end-mills in 1 vol% CuO nano-MQL condition after 450 mm cutting length	69
Fig. 4.18	Tool diameter reduction (%) with different cutting environments after 450 mm machining length	70
Fig. 4.19	The variation of cutting forces with machining length under different environments	72
	Micromilling feed forces for uncoated and AlTiN coated WC tools:	
Fig. 4.20	(a) & (b) for dry conditions, (c) & (d) for pure MQL (deionized water), (e) & (f) for 0.25 vol% CuO nanofluids MQL and, (g) & (h) for 1 vol% CuO nanofluids MQL conditions respectively	73
Fig. 4.21	The variation of average surface roughness with machining length by uncoated, AlTiN coated, and TiAlN coated WC micro end-mill in (a) dry (b) Pure MQL (c) 0.25 vol% CuO nanofluids MQL and (d) 1 vol% CuO nanofluids MQL conditions	75
Fig. 4.22	Micro-channel made by the uncoated WC tool in dry condition showing the workpiece feed direction, down milling and up milling sides, and burr width measurement	78
Fig. 4.23	Top burr width in up and down milling with different cutting environments between machining lengths of 405 mm and 450 mm	78
Fig. 4.24	The top view of SEM images of titanium alloy micro-slots was at the cutting distance between 405 mm and 450 mm for uncoated, AlTiN coated, and TiAlN coated WC micro-mills in dry condition, Pure MQL, CuO NF-MQL conditions with 0.25 vol% and 1 vol%	80
Fig. 4.25	SEM images and EDS analysis of machined surfaces lubricated with 1 vol% CuO nanofluids	81

Fig. 4.26	Surface topography images of micro-milled surface produced by uncoated, AlTiN coated, and TiAlN coated WC micro-mills under (a)-(c) dry condition and (d)-(f) Pure MQL condition.	82
Fig. 5.1	Experimental setup using a CNC micromachining center and MQL attachment	88
Fig. 5.2	SEM images of fresh AlTiN coated WC micro endmill (a) bottom view, (b) cutting edge radius, (c) side view	88
Fig. 5.3	Characterization of nanoparticles by TEM (a) & (b) CuO nanoparticles, (c) & (d) MoS ₂ nanosheets, and (e) & (f) hybrid CuO-MoS ₂ nanofluids	91
Fig. 5.4	XRD plots of (a) CuO and (b) MoS ₂ nanoparticles with SAED pattern of (c) CuO and (d) MoS ₂ nanoparticles showing polycrystalline rings	91
Fig. 5.5	Prepared nanofluids used in micromilling	92
Fig. 5.6	The dynamic viscosity of soybean oil and its nanofluids	93
Fig. 5.7	Droplet size measurement: (a) Droplet captured image, (b) 8-Bit mapping image, (c) Droplet size variation along with the number of counts, (d) Frequency distribution of droplet size	94
Fig. 5.8	Contact angle measurement	95
Fig. 5.9	Contact angle of (a) soybean oil and (b) CuO, (b) MoS ₂ nanofluids, and (d) CuO-MoS ₂ hybrid nanofluids	96
Fig. 5.10	(a) Trends of the coefficients of friction with time (b) Magnitude of coefficients of friction for different lubricating conditions	97

Fig. 5.11	SEM images of wear tracks under (a) & (b) dry, (c) & (d) soybean oil, (e) & (f) CuO nanofluids, (g) & (h) MoS ₂ nanofluids, and (i) & (j) hybrid CuO-MoS ₂ nanofluids lubricating conditions	98
Fig. 5.12	SEM images of WC micro mill at 0.3 μm/tooth feed after cutting distance of 250 mm under (a) dry, (b) soybean oil MQL, (c) CuO NF-MQL, (d) MoS ₂ NF- MQL, and (d) CuO-MoS ₂ NF-MQL	101
Fig. 5.13	EDS scans for AlTiN coated WC microtool at 0.3 μm/tooth feed in (a) & (b) dry, (c) CuO nanofluids MQL, and (d) hybrid CuO-MoS ₂ nanofluids MQL condition	102
Fig. 5.14	SEM images of WC micro mill at 4 μm/tooth feed after cutting distance of 250 mm under (a) dry, (b) soybean oil MQL, (c) MQL with CuO nanofluids, (d) MQL with MoS ₂ nanofluids, and (d) MQL with hybrid CuO-MoS ₂ nanofluids	104
Fig. 5.15	EDS scans for AlTiN coated WC microtool at 4 μm/tooth feed in (a) dry, (b) soybean oil MQL, (c) CuO nanofluids MQL, (d) MoS ₂ nanofluids MQL, and (e) hybrid CuO-MoS ₂ nanofluids MQL condition	105
Fig. 5.16	(a) % diameter reduction of tools and (b) enlargement in edge radius	106
Fig. 5.17	Typical cutting forces in micromilling (a) denotes three components cutting forces (b) feed force Vs. time and (c) cross-feed force Vs. time	109
Fig. 5.18	Variation of specific cutting force at feed (a) 0.3 μm/tooth and (b) 4 μm/tooth under different environmental conditions	110
Fig. 5.19	Scanning electron microscopy (SEM) image of top burr generation in Ti6Al4V	111

Fig. 5.20	Magnitude of equivalent burr width in (a) plowing zone and (b) shearing zone under different lubrication conditions	112
Fig. 5.21	Burr formation in plowing and shearing conditions with the cutting length in between 200 and 250 mm under different cutting environments	113
Fig. 5.22	Surface topography and surface roughness of the micro-slot mid-region at 0.3 $\mu\text{m}/\text{tooth}$ feed with the cutting length between 200 and 250 mm under different machining environments	116
Fig. 5.23	Surface topography and surface roughness of the micro-slot middle region at 4 $\mu\text{m}/\text{tooth}$ feed with the cutting length between 200 and 250 mm under different machining environments	117
Fig. 6.1	DT110 Micromachine with a close view of the MQL setup	122
Fig. 6.2	Prepared emulsions of soybean oil-water and paraffin oil-water	124
Fig. 6.3	Particle size distribution for (a)-(c) soybean oil-water emulsion and (b) paraffin oil-water emulsion	125
Fig. 6.4	Tribology setup	126
Fig. 6.5	Variation in the coefficient of friction at different lubricating conditions	126
Fig. 6.6	Variation of cutting forces with different cutting environments	127
Fig. 6.7	Feed force variation for dry and paraffin oil-water emulsion with different MQL flow rates	129
Fig. 6.8	Feed force variation for soybean oil-water emulsion with different MQL flow rates	130
Fig. 6.9	Typical SEM image denoting burr width measurement in down milling	131

Fig. 6.10	SEM images of top burr formation after up or down milling under dry conditions and paraffin oil-water emulsion with different MQL flow rates at 10000 rpm and 35000 rpm spindle speed	132
Fig. 6.11	SEM images of top burr formation after up or down milling under soybean oil-water emulsion with different MQL flow rates at 10000 rpm and 35000 rpm spindle speed	133
Fig. 6.12	Variations in down milling and up milling burr width at different spindle speeds under various lubricating conditions	135
Fig. 6.13	Surface profile of the machined channel for dry and paraffin oil-water emulsion environments with different MQL flow rates	136
Fig. 6.14	Surface profile of the machined channel for soybean oil-water emulsion environment with different MQL flow rates	137
Fig. 6.15	Variation of surface roughness with cutting environments	138

LIST OF TABLES

Table 1.1	Aspects of different micro-manufacturing processes	2-3
Table 2.1	Comparison of micro-milling and conventional macro milling cutters	10
Table 2.2	Overview of the lubrication mechanism of nanoparticles	30
Table 2.3	Influence of various cutting fluids and nanofluids in micromachining	33-35
Table 3.1	Mechanical properties of Ti6Al4V	40
Table 3.2	List of the instruments utilized during the experiment and characterizations with their images	44-46
Table 4.1	Mechanical properties and geometry of uncoated, AlTiN, and TiAlN coated WC micro-mills	49
Table 4.2	Micro-milling parameters and MQL conditions	51
Table 4.3	Lubrication conditions with different coated tools	52
Table 5.1	Geometry of end mill cutter	89
Table 5.2	Micromilling and MQL parameters	89
Table 5.3	Composition of the prepared nanofluids	90
Table 6.1	Micromilling and MQL parameters	123
Table 6.2	Physical properties of soybean oil	123

LIST OF ABBREVIATIONS/SYMBOLS

FIB	Focused ion beam
WEDM	Wire electric discharge machine
LIGA	Lithography-electroplating-molding
PLA	Pulsed laser ablation
MQL	Minimum quantity lubrication
PVD	Physical vapor deposition
MUCT	Minimum uncut chip thickness
RMS	Root mean square
P-V	Peak-to-valley
CVD	Chemical vapor deposition
DAQ	Data Acquisition System
WC	Tungsten carbide
SEM	Scanning electron microscope
EDS	Energy dispersive spectroscopy
XRD	X-Ray diffraction
TEM	Transmission electron microscope
DLS	Dynamic light scattering
SDS	Sodium dodecyl sulfate
NF-MQL	Nanofluids minimum quantity lubrication
COF	Coefficient of friction
CuO	Copper oxide
MoS ₂	Molybdenum disulfide
SO+DIW	Soybean oil-water emulsion
PO+DIW	Paraffin oil-water emulsion
AlTiN	Aluminum Titanium Nitride
TiAlN	Titanium Aluminum Nitride

Symbols used

mm	Millimeter
HV	Viker's Hardness
μm	Micrometer
θ	Theta
Sec	Second
Min	Minute
T	Temperature
F_x, F_y	Forces (N) in feed and perpendicular to feed directions
f_z	Feed per flute ($\mu\text{m}/\text{tooth}$)
n	Spindle speed (RPM)
d	Diameter of tool (mm)
Z_c	Number of flutes
$\gamma_{sv}, \gamma_{sl}, \gamma_{lv}$	Surface tension among solid-vapor, solid-liquid, liquid-vapor states
R_a	Roughness average
S_a	Arithmetical mean of the surface